

# Simulation Based Mask Defect Printability Verification and Disposition, Part II

Eric Guo, Irene Shi, Blade Gao and Nancy Fan

*Semiconductor Manufacturing International Corp., 18 Zhangjiang Road, Pudong New Area, Shanghai, China 201203*

Guojie Cheng<sup>a</sup>, Li Ling<sup>a</sup>, Ke Zhou<sup>a</sup>, Gary Zhang<sup>a</sup>, Ye Chen<sup>b</sup>, Chingyun Hsiang<sup>b</sup> and Bo Su<sup>b</sup>

<sup>a</sup>*Anchor Semiconductor, 668 East Beijing Road, East Building 19B, Shanghai, China 200001*

<sup>b</sup>*Anchor Semiconductor, 5403 Betsy Ross Drive, Santa Clara, CA 95054 USA*

## ABSTRACT

We have reported the first part of the work in 2009 BACUS meeting [1], using primarily SEM mask defect images as input. This paper is the extension of that work using mask optical inspection images with a new image process algorithm.

Simulation has been widely used in overall lithography process, called computational lithography, as an effective way for cost and time reduction. As the industry moves towards 45nm and 32nm technology nodes in production, the mask inspection, with increased sensitivity and shrinking critical defect size, catches more and more nuisance and false defects. Increased defect counts pose great challenges in the post inspection defect classification and disposition: which defects are real defects, and among the real defects, which defects should be repaired and how to verify the post-repair defects. In this paper, we report simulation mask defect printability check and disposition results extending beyond SEM mask defect images [1] into optical inspection mask defects images to demonstrate cost and time reduction by simulation in mask defect management area.

A new algorithm has been developed in the software tool to convert optical inspection mask defect images into “pseudo-defect” polygons in GDS format. Then, the converted defect polygons were filled with the correct tone to form mask patterns and were merged back into the original design GDS. With lithography process model, the resist contour of area of interest (AOI-the area surrounding a mask defect) can be simulated. If such complicated model is not available, a simple optical model can be used to get aerial image intensity of AOI. With build-in contour analysis functions, the software can easily compare the contour (or intensity) differences between real mask (with defect) and normal mask (without defect). With user provided judging criteria, software can be easily disposition the defect based on contour comparison.

The software has been tested and adapted for production use. We will present some accuracy test results against AIMS tool or wafer CDs in defect printability check.

Key words: Mask defects, optical image, simulation, defect repair, verification, disposition

## INTRODUCTION

Lithography process has been the driver of the technology advances in IC manufacturing for several decades and will continue to be so. Masks have been one of the most critical components in image transfer from design to silicon through lithography process since 130nm technology node and below. The cost of mask making has been increasing drastically and the trend is continuing and accelerating. For foundries, it is particularly important to control the costs associated with mask making processes. Previously, we presented a specifically developed, cost-effective software solution—SMDD (Simulation based Mask Defect Disposition) in mask defect handling; including defect printability check and defect post repair verification and disposition to reduce the need for costly hardware solutions using SEM based input. [1] In this paper, we report the extended SMDD capability using optical mask inspection images as input for the same purpose.

Similar work has been carried out by others recently [2-3] using optical mask inspection. The cost saving benefit of software solutions has been demonstrated already in production. The application flow of SMDD using optical images is actually simpler compared to that of SEM images as shown in Figure 1, since no additional SEM image taken step is needed. In this paper, we will focus on new capabilities associated with optical image input. All other related SMDD functions and GUI description have already been discussed previously. [1]

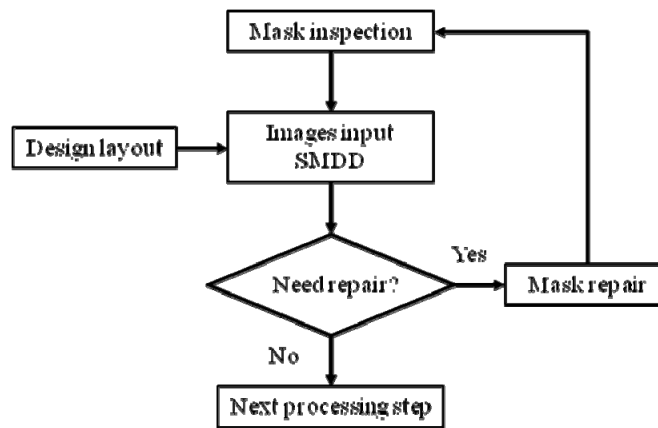


Figure 1: Basic SMDD flow with optical image input used in mask shop for defect disposition

## OPTICAL IMAGES

Optical images of mask defects from mask inspection systems are quite different compared to SEM images. The first and foremost is that optical images have much less resolution compared to SEM images, thus, the extracted contours from optical images are not very accurate representations of AOI around mask defects, as compared to SEM images. However, mask defect printability checking in wafer plane is quite forgiving in terms of defect detailed shapes, as long as the defect size and location can be extracted accurately. The reason of such forgiveness in defect detailed shapes is quite similar to small contact hole corner rounding (the same area of a square contact hole and a circle contact hole on mask will print the round contact holes with the same area on wafer plane)—the detailed shape information of a defect on mask in image transfer process from a mask to wafer in today's advanced technology nodes has been filtered out through optical Fourier transformation (a effective low pass filter). The key information needed for mask defect printability checking is good approximation of a defect in size and location (relative to its surrounding features). Thus, for optical images, the focus becomes how to extract defect location and size more accurately on mask.

Optical images have advantages over SEM images in two aspects for mask defect printability checking. First, optical images can have both transmitted and reflected images from mask inspection system. Second, optical images have a set of reference images in die-to-die defect detection algorithm. By utilizing multiple sets of optical images from a defect, a defect contour can be extracted relative accurately in defect size and

location. In addition, optical images contains information about film thickness (or phase related) induced mask defects, which complements SEM images' surface topography defect detection only limitation.

### APPLICATION FLOW

Extended SMDD uses mask inspection optical images and the corresponding design layout as input data. The software first loads in a mask inspection report (a KLARF file, which contains defect optical images). SMDD can load in multiple KLARF files, if needed. SMDD then does mask defect recognition and defect contour extraction, using all available optical images, including transmitted and reflected defect images, as well as transmitted and reflected reference images, if available. The extracted edge contours are then converted to GDSII format polygons as in layout designs, with polygon fill. Because the converted contours from optical images are not good representation of the mask except for defect itself, unlike in SEM image cases, SMDD uses the design around a defect, with addition of defect contour itself to represent the AOI on mask. The large enough area is included around a defect (AOI—area of interest) in simulation to ensure accuracy from optical proximity effect.

A lithography process model is loaded into the software before simulation. The same lithography model is used in OPC or OPC verification, created well before mask making step. If such complicated lithography process model is not available, a simple optical model can be also used. The software can simulate aerial image intensity profiles using the simple optical model with newly generated mask patterns. With a constant intensity threshold, lithography impact can be analyzed in SMDD. Simulation with a full lithography process model is preferred, since much more accurate wafer resist contours can be obtained.

Two wafer resist contours can be simulated and compared in the software. One is the resist contour of AOI with the converted mask patterns with the defect; and the other is a normal mask pattern without defect as a reference, similar to die-to-die referencing strategy. If it is desirable, the simulated resist contour of an ideal mask (design) can also be used as a reference, in analogy to die-to-database referencing strategy. A contour difference check can be performed within AOI and compared with user specified contour tolerances. A disposition judgment is then performed based on simulation contour comparison result and user specified tolerance specification, which then completes the mask defect printability verification and disposition. The above-mentioned flow is shown in Figure 2. The flow can be used to determine whether a mask defect needs repair, as well as to verify post-repair effectiveness.

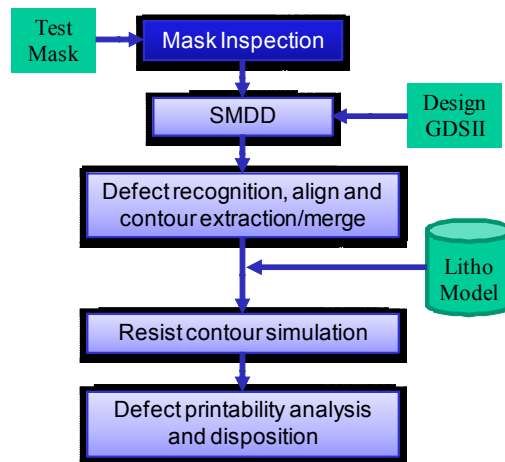


Figure 2: SMDD application flow of mask defect disposition.

The detailed description of SMDD software and its functions is given in reference [1]. In this paper, we will focus on functions and results related to optical images of mask defects.

### OPTICAL IMAGE PROCESSING

After loading the optical images into SMDD, users select “optical image mode” (the other mode is SEM image) for optical image processing. We will use a programmed defect to illustrate the working flow of optical image processing. Figure 3 shows some intermediate steps in SMDD optical image processing. There are several intermediate steps that SMDD takes before reaching the final converted GDS patterns of AOI with a detected defect. Those intermediate steps are transparent to the end users during normal operation. We show them here for illustration purpose only. First, SMDD does optical images and layout pattern alignment as shown in Figure 3 (a). The optical image used in the example is a reference image. It is a critical step to accurately place a defect relative to its surrounding features. Next, SMDD extracts the defect image contour and the reference image contour, then isolates the defect by comparing the defect and the reference contours as shown in Figure 3 (b) (the yellow shape). The optical image in Figure 3 (b) is a defect image. SMDD then completes the image processing by combining layout design and the extracted defect. Figure 3 (c) shows comparison between the final converted GDS format mask layout with a programmed defect and its corresponding SEM image. The zoom-in view of the defect region is shown in the upper right corner in Figure 3 (c). For this particular programmed defect, the converted mask pattern from optical images match the SEM image very well. After that, SMDD moves to simulation step after loading a lithography model.

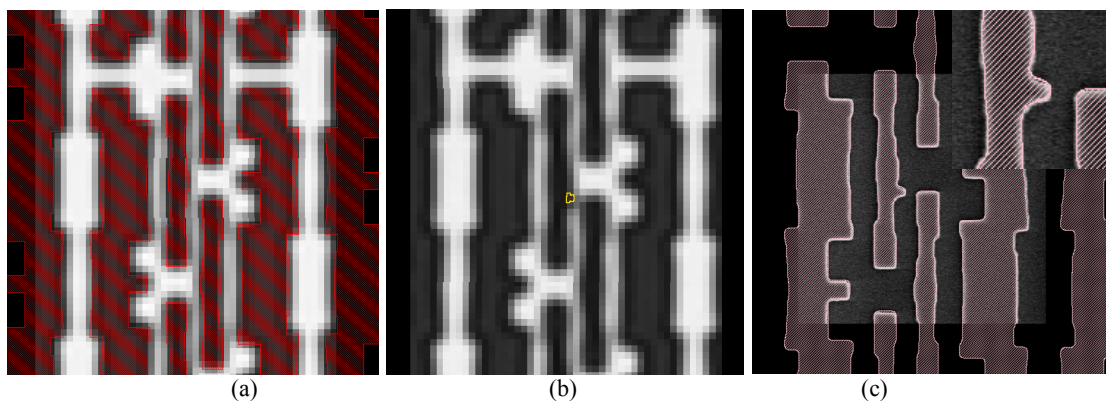


Figure 3: Illustration of intermediate SMDD optical image processing steps.

### ACCURACY OF SMDD WITH OPTICAL IMAGE INPUT

To demonstrate the validity of optical image in SMDD, we first use a test mask with programmed defects to compare SMDD simulated results and SMIC’s reference results. The reference results can be either AIMS system measurements or direct wafer CD measurements. The test mask uses SMIC 45/40nm technology and consists of various test patterns and pseudo-circuit patterns. It has both line/space type defects and contact/via type of defects with various defect sizes. Multiple critical layer substrate wafers were processed using the corresponding layer process conditions. Production CD measurement recipe is used for wafer CD measurements.

Figure 4 shows the summary of direct comparison of SMDD extracted results of line/space type of programmed defects and their corresponding SEM images at mask plane. Figure 5 shows the summary of direct comparison of SMDD extracted results of contact/via type of programmed defects and their corresponding SEM images at mask plane. Even though, in sub-wavelength photo-lithography, the reconstruction of exact shape of a defect is not critical (the high-frequency components of a defect in Fourier domain, which corresponding to sharp corners of a defect are filtered out in imaging process) in mask defect printing check, we still want to show such direct comparison for validity of optical image reconstruction. The rounding of the sharp ends of a defect in SMDD re-constructed mask layout is clearly seen in Figure 4 (b) for the third defect, which is intrinsically the limitation of optical images in mask pattern reconstruction, due to the missing information of high frequency Fourier spectrum in mask inspection images. However, as we pointed out before, such rounding may not be matter in mask defect printing check, as long as the re-constructed defect contains all necessary imaging Fourier frequency

spectrum for sub-wavelength printing. In advanced technology nodes using 193nm exposure wavelength, such condition is sufficiently met.

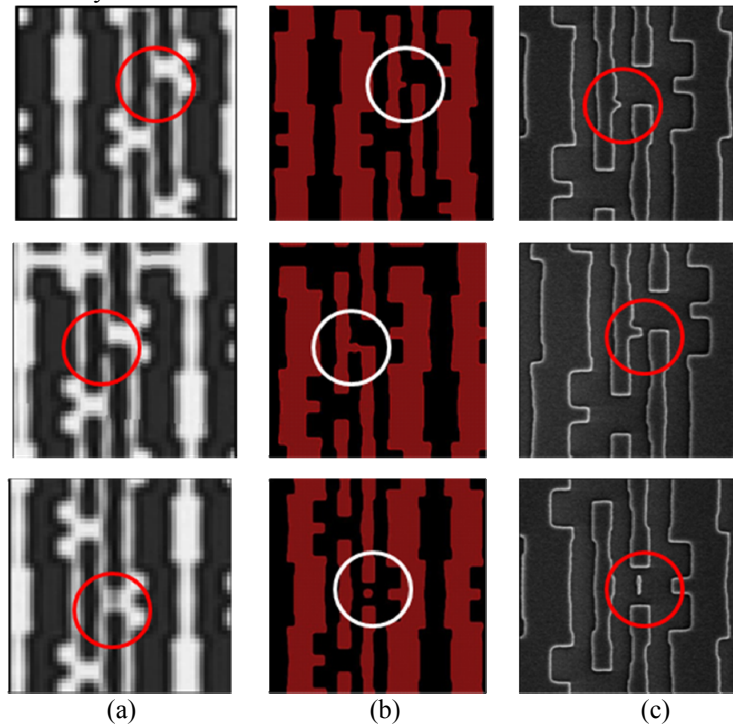


Figure 4: the one of transmitted optical images (a); SMDD re-constructed mask pattern near the defect (b) and the SEM image for three line/space types of programmed defects.

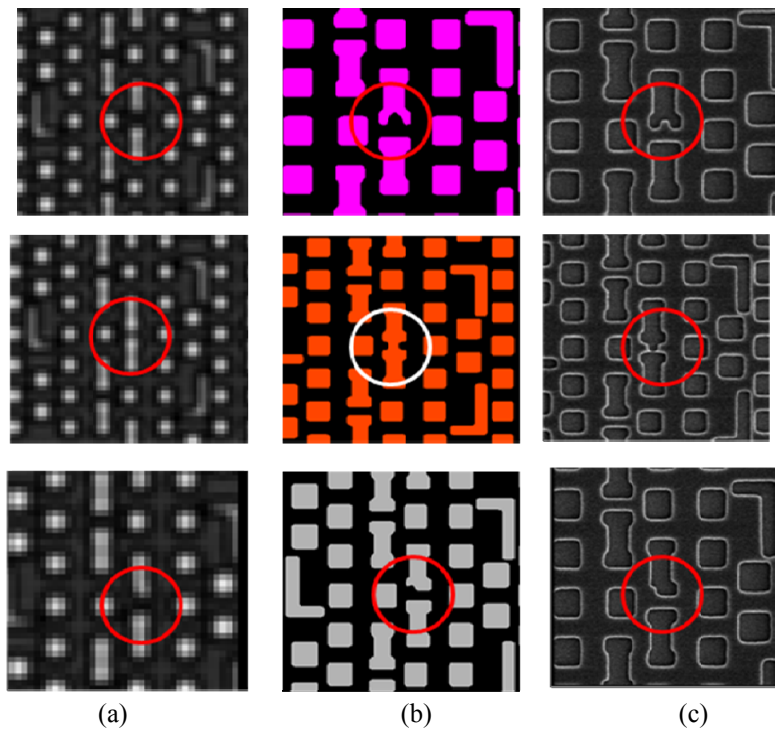


Figure 5: the one of transmitted optical images (a); SMDD re-constructed mask pattern near the defect (b) and the SEM image for three contact/via types of programmed defects.

Next, we check CD matching between SMDD simulated CDs from programmed defects and direct wafer CD measurements. SMDD uses full lithography models for simulation in such direct CD comparison. Figure 6 shows systematic CD comparison between SMDD simulation and wafer CD measurements for 4 programmed defect types. As one can see, the SMDD simulated CDs match the wafer CD measurements well. The CD match for the contact type programmed defects shows relatively large errors. We contribute that to two factors: one is increased defect impact in contact CD; and the other is increased CD measurement error for contact CD (measurement location errors and relative high measurement noise) by CD SEM.

The good CD matching confirmed the validity of optical images as input in SMDD.

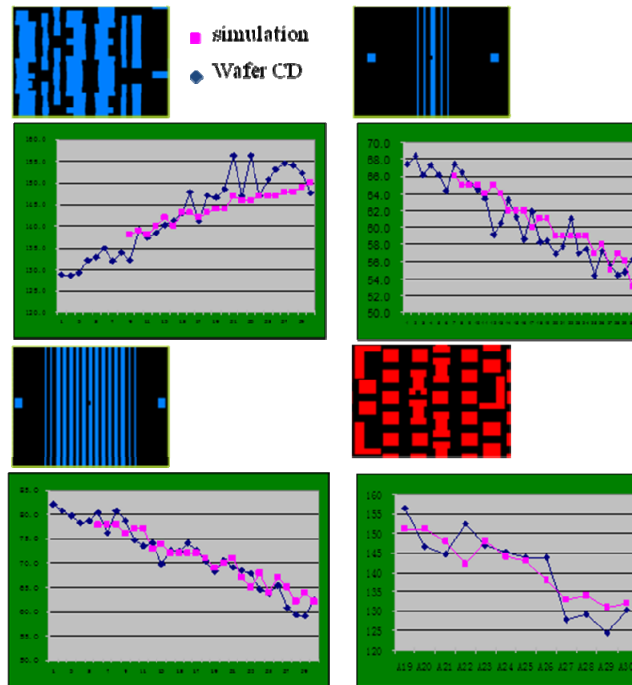


Figure 6: the systematic CD comparison data from 4 different programmed defects (as shown on top of each charts). The data shows good agreement between the SMDD simulation's prediction and actual wafer CD measurements.

## ANALYSIS AND DISPOSITION

Similar to SEM image mode in SMDD, after simulation, it comes to the final analysis and disposition step. With OPC model, the analysis is straightforward—directly checking feature CD change at the defective location between defective mask pattern and a normal mask pattern. While with simple optical model, the analysis requires additional steps. The analysis starts with aerial image intensity. Figure 7 shows the analysis and disposition GUI and it contains 6 sections in the analysis GUI from left to right and top to bottom matrix: Area Intensity Maps from two optical images—a defective image and a reference image; Location-Intensity Chart (user selected analysis line); Area Contour Map; Threshold-Width Chart; Focus-NILS Chart (requires defocus model); and Area optical images (for reference). Additional intensity file can be loaded in and displayed in this GUI. After user selects an analysis line (the white line in top-left intensity image in Figure 7), two intensity curves are shown in the Location-Intensity Chart: one from the defective optical images and another from a reference image. A constant threshold can be placed in Location-Intensity Chart and corresponding CD vs. Threshold curves are displayed in Threshold-Width Chart window and the CD values at the selected threshold will be highlighted and shown on top of the chart. By clicking on the Delta motif icon on top, the CD delta will be displayed. By connecting any two edges using mouse drag, CD values between the two edges will be shown. Without defocus models, only one point from each masks will displayed in Focus-NILS Chart. With defocus models, a focus-NILS chart will be displayed. The intensity profile can be saved and loaded back later for further analysis. Disposition decision is made on the top of the screen by selecting PASS, FAIL, or PENDING.

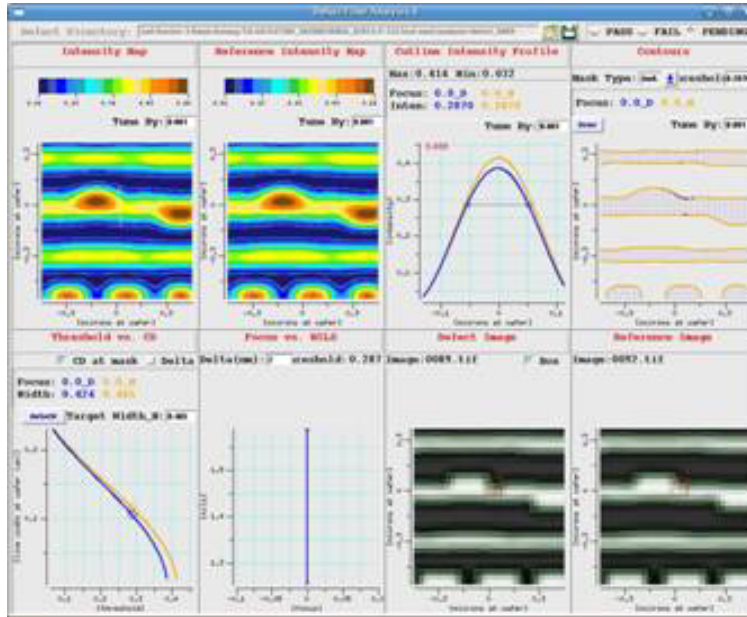


Figure 7: SMDD analysis and disposition screen for optical image input. Notice the multiple optical images in the GUI.

### ACCEPTANCE TEST

With extended optical image processing capability, SMIC mask-shop conducted a systematic acceptance test on SMDD against its existing references with AIMS and wafers. The test covers three areas: SMDD simulation accuracy; processing speed and ease of use. SMDD passes all acceptance test specifications in three areas. Since SMDD can do parallel processing, speedup overall performance can be achieved with more CPUs. In addition, SMDD has improved greatly in automation. After initial tuning for a given mask plate type, a fully automated SMDD flow has achieved and used routinely. Table 1 shows the overall CD matching summary of SMDD against AIMS measurements in AA/metal layers and contact layer. Again, CD match in contact/via layer shows relatively large error for the reasons mentions above.

CD match	AA/Metal	CT/Via
average	0.49%	1.48%
3 sigma	2.53%	6.60%

Table 1: CD matching summary of SMDD simulation vs. AIMS measurements.

With added capability in optical image processing and improvement in automation, SMDD has been tested and adopted in production use in multiple sites in SMIC, to take advantages the cost saving and technology extendibility of software solution.

### SUMMARY

We have demonstrated a working software solution SMDD in mask defect printability check and mask defect post repair verification using optical images and design as inputs. The extended optical image processing complements SMDD's SEM image capability and makes SMDD a more complete software solution in mask defect analysis and disposition. With programmed defects on an advanced test mask, SMDD simulation accuracy has been rigorously tested using both wafer CDs and AIMS measurements. SMDD has been used in production and compared to the existing baseline hardware solution with satisfactory results. Improved automation of SMDD proves its production worthiness.

SMDD with optical images as input simplifies the application flow and is the default working mode. It offers maskshop a unique capability for mask defect analysis and disposition in R&D, as well as in production.

It is our believe that SMDD may be extended beyond what we described in the publications, in particular with combination of other software tools, to make mask defect inspection, mask defect classification and filtering more efficient.

## REFERENCES

- [1] Eric G. Guo, *et al*, “Simulation based mask defect repair verification and disposition”, Proc. SPIE **7488**, (2009).
- [2] Jin-Hyung Park, *et al*, “Mask Pattern Recovery by Level Set Method based Inverse Inspection Technology (IIT) and its Application on Defect Auto Disposition”, Proc. SPIE **7488**, (2009).
- [3] George Chen, *et al*, “Defect Printability Analysis by Lithographic Simulation from High Resolution Mask Images”, Proc. SPIE **7488**, (2009).